

Plasmon and shear modes in correlated superlattices

Kenneth I. Golden

Department of Mathematics and Statistics, University of Vermont, Burlington, Vermont 05401-1455

G. Kalman

Department of Physics, Boston College, Chestnut Hill, Massachusetts 02167

Limin Miao and Robert R. Snapp

Department of Computer Science and Electrical Engineering, University of Vermont, Burlington, Vermont 05405

(Received 6 March 1997)

The dynamical matrix, dielectric response tensor, and dispersion relations for a strongly correlated unmagnetized superlattice are formulated in the quasilocalized charge approximation. Analysis of the dispersion relations at wavelengths long compared with the spacing d between adjacent layers indicates that the random-phase-approximation (RPA) collective-mode structure is substantially modified by particle correlations. In earlier works [see, e.g., G. Kalman, Y. Ren, and K. I. Golden, *Phys. Rev. B* **50**, 2031 (1994)] the authors reported the existence of a long-wavelength energy gap in the acoustic plasmon band generated by strong interlayer correlations. The present analysis indicates the existence of a gapped shear mode band which is wholly maintained by Coulombic interlayer interactions over and above the RPA. When interlayer interactions are taken into account only through the average RPA field, the band collapses into a single shear mode which exhibits the long-wavelength acoustic dispersion characteristic of the correlated two-dimensional electron liquid. Other interesting effects include (i) an optical-phonon crystal-like dispersion exhibited by the in-phase plasmon at long wavelengths for d sufficiently small; and (ii) an acoustic-phonon dispersion exhibited by the in-phase shear mode at long wavelengths. [S0163-1829(97)08324-0]

I. INTRODUCTION

Over the past few years there has been considerable interest in the collective-mode behavior of layered electron systems in highly correlated states. The layered system to be addressed in this paper is the unmagnetized semiconductor superlattice consisting of a large number of identical two-dimensional (2D) electron plasma monolayers, each in a strongly correlated liquid phase. The spacing d between adjacent lattice planes is taken to be comparable with or less than the inplane 2D Wigner-Seitz radius a ; thus the *interlayer* Coulomb coupling is also strong.

Recent theoretical studies¹⁻⁶ of collective modes in layered electron systems indicate that particle correlations bring about substantial modifications in the RPA (random-phase approximation) (Ref. 7) plasmon dispersion. Our own studies³⁻⁶ indicate that for sufficiently high values of the *intralayer* coupling parameter $r_s = a/a_B^*$ (a_B^* is the effective Bohr radius), interlayer correlations transform the superlattice band of acoustic plasmon modes⁷ into a band of gapped modes,³⁻⁶ that is, into modes having finite oscillation frequencies at $k=0$ (k is the in-plane wave number). This is consistent with recent phonon spectrum calculations for the bilayer crystal with fixed interlayer spacing^{8(a),8(b)} and for the bilayer crystal with variable interlayer spacing in a wide quantum well^{8(c)} or in an ionic trap:^{8(b)} all of these calculations indicate a gapped dispersion for the out-of-phase longitudinal mode.

Our preliminary study^{4(e)} reveals that the correlated electronic superlattice, similarly to other strongly correlated plasmas, also supports transverse modes: an in-phase acoustic

shear mode and a band of gapped shear modes. Again, this is consistent with phonon spectrum calculations for the bilayer crystal;⁸ all indicate an in-phase transverse acoustic mode and a gapped dispersion for the out-of-phase transverse mode.

In the present paper we demonstrate that when interlayer interactions are taken into account only through the average RPA field, the superlattice shear band and in-phase mode collapse into a single acoustic shear mode characteristic of the isolated 2D electron layer in a correlated liquid phase.⁹ Thus it is the interlayer Coulomb correlations over and above the RPA which maintain the in-phase acoustic shear mode and gapped shear band as distinct entities.

In order to analyze modes with polarizations other than longitudinal, one has to generalize the Ref. 6 microscopic derivation of the 2D dielectric response function for the correlated unmagnetized superlattice. This is the first goal of this paper. The derivation is to be carried out in the quasilocalized charge approximation (QLCA),¹⁰ which is especially well suited to plasmas in the strongly correlated liquid state; the QLCA has already been used in the analysis of 2D, 3D, and superlattice systems.^{6,9-11} The method is based on a microscopic model in which the particles are quasilocalized on a short-time scale in local potential fluctuations; while the theory is built on an essentially classical picture, it is expected to be a reliable approach for quasilocalized electrons in degenerate electron liquid systems as well.

In the QLCA derivation of Ref. 6, we considered only the Coulomb interaction between the particles, and, correspondingly, we calculated the linear response to an external scalar potential perturbation. The second goal of this paper is to

extend the formalism beyond the usual quasistatic approximation, and to incorporate the full retarded character of the electromagnetic interaction. We find it useful to pursue this calculation here, partly to put the calculation of the transverse modes on a solid foundation, partly to pave the way for the analysis of the full electromagnetic spectrum of collective modes that will be the subject of a forthcoming publication.¹² Thus (i) by taking account of the full electromagnetic interaction and (ii) by calculating the linear response to combined external scalar and vector potential perturbations, the nonretarded scalar response formalism of Ref. 6 is generalized to a retarded 2D tensor response formalism in the present work.

The ultimate goal of this paper is to analyze the long-wavelength ($kd \ll 1$) collective-mode dispersion in the nonretarded ($c_s \rightarrow \infty$) limit; c_s is the speed of light in the dielectric substrate. The present collective mode analysis extends that of Ref. 6 in three ways. (i) We establish the crystal-like dispersion of the in-phase (bulk) plasmon mode for sufficiently strong interlayer-coupling. (ii) A complete analysis of the shear mode dispersion is presented: we establish the transverse acoustic phononlike dispersion of the in-phase (bulk) shear mode, we formulate the mode frequencies for the gapped shear band, and we show that the bulk mode and band are maintained as separate entities by non-RPA interlayer correlations. (iii) In our previous studies³⁻⁶ only the intralayer (00) and nearest interlayer (± 10) static structure functions appear in the expressions for the mode frequencies; here we display the *complete* hierarchy of superlattice layer-layer ($m0$) ($m=0, \pm 1, \pm 2, \dots$) static structure functions. (iv) We establish the connection between the formalism appropriate for the periodic superlattice and the formalism for an anisotropic three-dimensional medium.

The collective-mode analysis of the present paper focuses primarily on correlational effects. Insofar as the plasmon and shear modes are concerned, one can justifiably ignore electrodynamic retardation effects on the grounds that displacement currents are almost always dominated by the electrostatic effects of nearby layers. Analysis of these modes at the exceedingly small wavenumbers $\approx \omega/c_s$ where displacement currents would have to be taken into account, and the concomitant analysis of the higher-frequency electromagnetic modes,¹³ calls for a separate treatment to be presented in a later work¹² which implements the QLCA retarded 2D tensor response formalism of the present paper.

The organization of the paper is as follows. In Sec. II we calculate the dynamical matrix and the dielectric response tensor in the QLCA,¹⁰ and we set up the dispersion relation. All the intralayer and interlayer correlational effects appear quite naturally as local-field corrections in the elements of the dielectric tensor; the quasistatic limit ($c_s \rightarrow \infty$) of the Coulomb correction has been identified as the correlational contribution to the third-frequency-moment sum-rule coefficient.^{6,14} In Sec. III we recast the local-field corrections in a form which explicitly features the hierarchy of intralayer and interlayer correlational components and static structure functions. We then evaluate the correlational components in the quasistatic limit and in the long-wavelength regime, thus paving the way for the Sec. IV analysis of the long-wavelength collective-mode dispersion. Reiterating our goal here, we wish to understand how intralayer and interlayer

Coulomb correlations affect the in-phase and the gapped band of shear modes, and how the in-phase (longitudinal) plasmon and (transverse) shear modes in a superlattice compare with their respective optical and acoustic phononlike counterpart modes in the strongly coupled 3D OCP.^{11(b),15,16} In Sec. V we discuss the dielectric formalism for an anisotropic medium and its equivalence in the long-wavelength limit to the more general treatment pursued earlier in the paper. Conclusions are drawn in Sec. VI.

II. DYNAMICAL MATRIX AND DIELECTRIC TENSOR

Consider the infinite, type-I superlattice model consisting of a large stack of N_L electron-plasma monolayers, each of area A and parallel to the xy plane; the monolayers are embedded in a dielectric substrate; $L = N_L d$ is the length of the superlattice, d being the spacing between adjacent planes; $a = 1/\sqrt{\pi n_s}$ is the 2D Wigner-Seitz radius, $n_s = N_e/A$ being the average areal density of each monolayer. The intralayer coupling strength is characterized by the parameter $r_s = a/a_B^*$, which is the average spacing between electrons in units of the effective Bohr radius, or by its classical equivalent $\Gamma = \beta e^2/(a\epsilon_s)$, ϵ_s being the substrate dielectric constant and $1/\beta$ the electron temperature in energy units. The corresponding interlayer coupling parameters are $r_s(a/d)$ or $\Gamma(a/d)$.

We wish to calculate the linear response to small external scalar and vector potentials $\hat{\Phi}$ and $\hat{\mathbf{A}}$ beyond the RPA, taking full account of electrodynamic retardation effects. Following the general scheme of the QLCA, we derive the expression for the dynamical matrix \mathbf{C} that controls the dynamics of the average induced current response. We begin by constructing the coupled linearized microscopic equations of motion describing the rapid oscillations of the charges about their slowly drifting quasiequilibrium site positions. Let $\mathbf{x}_{i,m}(t) = \mathbf{x}_{i,m} + \xi_{i,m}(t)$ be the momentary position of the i th particle in the m th lattice plane, $\mathbf{x}_{i,m}$ its quasiequilibrium site position, and $\xi_{i,m}(t)$ the perturbed amplitude of its small excursion (indices i, j and m, n enumerate particles and layers, respectively). The microscopic equation of motion for particle i in layer m can now be written as follows:

$$\begin{aligned} & -m^* \omega^2 \xi_{i,m}(\omega) + \sum_j \sum_n \mathbf{K}_{ij,mn}(\omega) \cdot [\xi_{j,n}(\omega) - \xi_{i,m}(\omega)] \\ & + \sum_j \sum_n \mathbf{M}_{ij,mn}(\omega) \cdot \xi_{j,n}(\omega) \\ & = -e \hat{\mathbf{E}}_m(\mathbf{x}_{i,m}, \omega) = -\frac{e}{A} \sum_{\mathbf{k}} \hat{\mathbf{E}}_m(\mathbf{k}, \omega) e^{i\mathbf{k} \cdot \mathbf{x}_{i,m}}, \end{aligned} \quad (1)$$

where m^* is the effective electron mass, $\hat{\mathbf{E}}_m(\mathbf{x}_{i,m}, \omega)$ is the lattice-plane component of the external electric field acting at the field point $(\mathbf{x}_{i,m}, z_m \equiv md)$, and $\hat{\mathbf{E}}_m(\mathbf{k}, \omega) = (i\omega/c_s) \hat{\mathbf{A}}_m(\mathbf{k}, \omega) - i\mathbf{k} \hat{\Phi}_m(\mathbf{k}, \omega)$ is its in-plane Fourier transform, \mathbf{k} being the wave vector parallel to the xy plane. The $\mathbf{K}_{ij,mn}(\omega)$ term contains the effects of the longitudinal Coulomb interaction between the particles

$$\mathbf{K}_{ij,mn}(\omega) = \frac{1}{A} \sum_{\mathbf{k}} \mathbf{L}(\mathbf{k}) k^2 \psi_{mn}(k, \omega) e^{i\mathbf{k} \cdot (\mathbf{x}_{i,m} - \mathbf{x}_{j,n})}, \quad (2)$$

while the $\mathbf{M}_{ij,mn}(\omega)$ term originates from the transverse retarded electromagnetic interaction

$$\begin{aligned} \mathbf{M}_{ij,mn}(\omega) &= \frac{1}{A} \sum_{\mathbf{k}} \mathbf{T}(\mathbf{k}) k^2 \psi_{mn}(k, \omega) e^{i\mathbf{k} \cdot (\mathbf{x}_{i,m} - \mathbf{x}_{j,n})} \\ &\quad \times \left(\frac{1 - \delta_{ij} \delta_{mn}}{1 - (kc_s/\omega)^2} \right), \end{aligned} \quad (3)$$

$$\psi_{mn}(k, \omega) = \frac{2\pi e^2}{\varepsilon_s k^2} \beta_s(k, \omega) e^{-\beta_s(k, \omega) |m-n|d} \quad (4)$$

is the layer m -layer n effective potential $\mathbf{L}(\mathbf{k}) = \mathbf{k} \cdot \mathbf{k} / k^2$ and $\mathbf{T}(\mathbf{k}) = \mathbf{I} - \mathbf{k} \cdot \mathbf{k} / k^2$ are notationally convenient longitudinal (L) and transverse (T) projection tensors in the xy plane, and \mathbf{I} is the unit tensor in the xy plane. Note the appearance of $\beta_s = [k^2 - \omega^2/c_s^2]^{1/2}$ in Eq. (4): this is the z component of the propagation vector; real values of β_s describe exponentially decaying, i.e., nonpropagating behavior of the lattice

planes, while imaginary β_s values correspond to a propagating behavior in the interlayer regions. Even though the notation of Eq. (4) is appropriate for the nonpropagating ($k > \omega/c_s$) sector of the ω - k plane, there is no difficulty in analytically continuing (with $\beta_s \rightarrow i\kappa = i[(\omega/c_s)^2 - k^2]^{1/2}$) into the propagating ($k < \omega/c_s$) sector. In the quasistatic limit ($c_s \rightarrow \infty$), we observe that $\beta_s = k$, $\mathbf{M}_{ij,mn}(\omega) = 0$, and $\psi_{mn}(k, \omega) = \phi_{2D}(k) \exp(-k|m-n|d)$, where $\phi_{2D}(k) = 2\pi e^2/(\varepsilon_s k)$ is the Fourier transform of the 2D Coulomb potential $\phi_{2D}(r) = e^2/(\varepsilon_s r)$, r being the in-plane separation distance. Returning to the more general case where electromagnetic interaction and displacement current effects are fully retained, we note that, in the $d \rightarrow \infty$ limit, only the $m = n$ contribution to Eq. (1) survives, and that one recovers the QLC microscopic equation for the isolated 2D electron plasma monolayer.^{9,11(c)}

The calculation of the average particle current-density response \mathbf{j} and dynamical matrix \mathbf{C} from Eqs. (1)–(3) is carried out by implementing the general QLC formalism of Ref. 10. We obtain the equations of motion for the collective coordinate $\hat{\xi}_{\mathbf{k}}$:

$$[\omega^2 \mathbf{I} - \mathbf{C}(\mathbf{k}, q, \omega)] \cdot \hat{\xi}_{\mathbf{k}}(\omega) = \frac{e}{m} \hat{\mathbf{E}}(\mathbf{k}, q, \omega), \quad (5)$$

$$\mathbf{C}(\mathbf{k}, q, \omega) = \omega_{2D}^2(k) \left\{ \mathbf{L}(\mathbf{k}) \frac{\beta_s(k, \omega)}{k} F(\beta_s(k, \omega), q) - \mathbf{T}(\mathbf{k}) \frac{\omega^2}{k \beta_s(k, \omega) c_s^2} F(\beta_s(k, \omega), q) + \mathbf{D}(\mathbf{k}, q, \omega) + \mathbf{Q}(\mathbf{k}, q, \omega) \right\}; \quad (6)$$

$\omega_{2D}(k) = [2\pi n_s e^2 k / (\varepsilon_s m^*)]^{1/2}$ is the 2D plasma frequency, and m^* the effective mass; q is a wave number perpendicular to the lattice planes (but *not* the third component of the wave vector \mathbf{k}), and

$$\hat{\mathbf{E}}(\mathbf{k}, q, \omega) = \sum_m \hat{\mathbf{E}}_m(\mathbf{k}, \omega) e^{-iqmd} \quad (7)$$

is the layer-space Fourier transform of the external electric field $\hat{\mathbf{E}}_m(\mathbf{k}, \omega)$. The well-known superlattice form factor

$$F(\beta_s(k, \omega), q) = \frac{\sinh[\beta_s(k, \omega)d]}{\cosh[\beta_s(k, \omega)d] - \cos qd} \quad (8)$$

is the layer-space Fourier transform of the potential modifier $\exp[-\beta_s(k, \omega)|m-n|d]$, viz.

$$F(\beta_s(k, \omega), q) = \sum_m \exp[-\beta_s(k, \omega)|m-n|d] e^{-iq(m-n)d}, \quad (9)$$

$\exp[-\beta_s(k, \omega)|m-n|d]$

$$= \frac{1}{N_L} \sum_{|q| \leq \pi/d} F(\beta_s(k, \omega), q) e^{iq(m-n)d}, \quad (10)$$

with q defined only in the first Brillouin zone $|q| \leq \pi/d$ due to the invariance of the superlattice with respect to translation along the z axis by any lattice number $(2\pi/d) \times \text{integer}$. The first two right-hand-side terms of Eq. (6) represent the effects of the RPA on the dynamics. The third right-hand-side term

$$\begin{aligned} \mathbf{D}(\mathbf{k}, q, \omega) &= \frac{1}{k N_e N_L} \sum_{\mathbf{k}'} \sum_{|q'| \leq \pi/d} \mathbf{L}(\mathbf{k}') \beta_s(k', \omega) \\ &\quad \times F(\beta_s(k', \omega), q') [S(|\mathbf{k} - \mathbf{k}'|, q - q') \\ &\quad - S(k', q')] \end{aligned} \quad (11)$$

represents the important correlation-induced Coulomb part of the dynamical matrix; $S(k, q)$ is the layer-space Fourier transform of $S_{mn}(k)$, the layer m -layer n static structure function; the two are related by

$$S(k, q) = \sum_m S_{|m|0}(k) e^{-iqmd}, \quad (12)$$

$$S_{|m|0}(k) = \frac{1}{N_L} \sum_{|q| \leq \pi/d} S(k, q) e^{iqmd}, \quad (13)$$

where the zero subscript refers to an arbitrarily chosen reference layer. The fourth right-hand-side term of Eq. (6),

$$\mathbf{Q}(\mathbf{k}, q, \omega) = -\left(\frac{\omega}{c_s}\right)^2 \frac{1}{kN_e N_L} \sum_{\mathbf{k}'} \sum_{|q'| \leq \pi/d} \mathbf{T}(\mathbf{k}') \frac{1}{\beta_s(k', \omega)} \times F(\beta_s(k', \omega), q') [S(|\mathbf{k}-\mathbf{k}'|, q-q') - 1], \quad (14)$$

represents the correlation-induced electromagnetic contribution. The expressions for the longitudinal (L) and transverse (T) elements of \mathbf{D} and \mathbf{Q} are then calculated from Eqs. (11) and (14) and the tensor decompositions $\mathbf{D}(\mathbf{k}, q, \omega) = \mathbf{L}(\mathbf{k})D^L(\mathbf{k}, q, \omega) + \mathbf{T}(\mathbf{k})D^T(\mathbf{k}, q, \omega)$ and $\mathbf{Q}(\mathbf{k}, q, \omega) = \mathbf{L}(\mathbf{k})Q^L(\mathbf{k}, q, \omega) + \mathbf{T}(\mathbf{k})Q^T(\mathbf{k}, q, \omega)$.

The superlattice electrodynamics has been formulated entirely in terms of lattice plane field quantities in Ref. 17. Within this strictly layer-space framework, a dielectric response tensor $\epsilon_{mn}(\mathbf{k}, \omega)$ and its Fourier transform $\epsilon(\mathbf{k}, q, \omega)$ can be introduced in relation to lattice plane field quantities only and in terms of an ‘‘external’’ conductivity tensor $\hat{\sigma}_m(\mathbf{k}, q, \omega)$ defined by the constitutive relation (16) of Ref. 17. With this constitutive relation, the QLCA external conductivity can be readily extracted from Eq. (5). The longitudinal and transverse elements of $\epsilon(\mathbf{k}, q, \omega)$ are then calculated to be

$$\epsilon^\alpha(\mathbf{k}, q, \omega) = \epsilon_s \left\{ 1 - \frac{\omega_{2D}^2(k) \frac{\beta_s(k, \omega)}{k} F(\beta_s(k, \omega), q)}{\omega^2 - \omega_{2D}^2(k) [D^\alpha(\mathbf{k}, q, \omega) + Q^\alpha(\mathbf{k}, q, \omega)]} \right\} \quad (\alpha = L, T). \quad (15)$$

The eigenfrequencies $\omega(\mathbf{k}, q)$ for the collective modes then follow from Eq. (15) and the dispersion formulas¹⁷

$$\epsilon^L(\mathbf{k}, q, \omega) = 0, \quad (16)$$

$$\epsilon^T(\mathbf{k}, q, \omega) = (kc/\omega)^2. \quad (17)$$

The observation that in-plane electric-field excitations associated with dispersion relation (16) are polarized along \mathbf{k} requires that $B_z = 0$ in order to satisfy Maxwell’s equations. On the other hand, the in-plane electric-field excitations associated with Eq. (17) are polarized perpendicular to \mathbf{k} , so that Maxwell’s equations require $E_z = 0$ (for β_s^2 different from zero). It is therefore appropriate to refer to Eqs. (16) and (17) as the ‘‘TM’’ (transverse magnetic) and ‘‘TE’’ (transverse electric) dispersion relations, respectively. This we do in the sequel.

Alternatively, the knowledge of the dynamical matrix en-

ables one to formulate the dispersion relation directly from Eqs. (5) and (6). One readily obtains

$$\text{Det} \left\{ \omega^2 \mathbf{I} - \mathbf{C}(\mathbf{k}, q, \omega) \right\} = \left\{ \omega^2 - \omega_{2D}^2(k) \left[\frac{\beta_s(k, \omega)}{k} F(\beta_s(k, \omega), q) + D^L(\mathbf{k}, \omega) + Q^L(\mathbf{k}, q, \omega) \right] \right\} \left\{ \omega^2 + \left(\frac{\omega}{c_s}\right)^2 \frac{\omega_{2D}^2(k) F(\beta_s(k, \omega), q)}{k \beta_s(k, \omega)} - \omega_{2D}^2(k) [D^T(\mathbf{k}, \omega) + Q^T(\mathbf{k}, q, \omega)] \right\} = 0. \quad (18)$$

The two (longitudinal and transverse) dispersion relations (16) and (17), in conjunction with Eq. (15), are identical to the dispersion relation (18).

III. QUASISTATIC APPROXIMATION AND LAYER-SPACE AND REPRESENTATION

The genuine collective modes of the superlattice are well described by ignoring retardation effects: this is the quasistatic approximation, whose philosophy and limitations were alluded to in Sec. I and in the text below Eq. (27). This approximation amounts to (a) simplifying the correlational $\mathbf{D}(\mathbf{k}, q, \omega)$ and $\mathbf{Q}(\mathbf{k}, q, \omega)$ contributions, and (b) omitting the electromagnetic \mathbf{Q} contribution entirely. The main purpose of this paper is to analyze the collective modes of the superlattice system in a quasistatic approximation. While the full electromagnetic treatment provides a complete description of all the modes in the system, including those which are merely electromagnetic waves modified by the presence of the superlattice, the physical significance of the quasistatic approximation is that it allows to survive only those modes which are genuinely collective, in the sense that they are maintained by particle-particle interaction.

To implement the quasi-static approximation we observe that for frequencies $\omega \ll c_s/d$, the correlation-induced Coulomb and electromagnetic contributions (11) and (14) are well approximated by replacing $\beta(k', \omega)$ by k' , i.e. by

$$\mathbf{D}(\mathbf{k}, q) = \frac{1}{kN_e N_L} \sum_{\mathbf{k}'} \sum_{|q'| \leq \pi/d} \mathbf{L}(\mathbf{k}') k' F(k', q') \times [S(|\mathbf{k}-\mathbf{k}'|, q-q') - S(k', q')], \quad (19)$$

$$\mathbf{Q}(\mathbf{k}, q, \omega) = -\left(\frac{\omega}{c_s}\right)^2 \frac{1}{kN_e N_L} \sum_{\mathbf{k}'} \sum_{|q'| \leq \pi/d} \mathbf{T}(\mathbf{k}') \frac{1}{k'} \times F(k', q') [S(|\mathbf{k}-\mathbf{k}'|, q-q') - 1]. \quad (20)$$

This can be seen by dividing the k' sum in Eqs. (11) and (14) into two sums, the first going from $k'=0$ to $k'=\omega/c_s$, and the second from $k'=\omega/c_s$ to $k'=\infty$. We note that $\beta_s(k', \omega) \approx k'$ over most of the far wider subinterval $[\omega/c_s, \infty)$. This same approximation holds as well for $k'd \in [0, \omega/c_s]$, because the interval is exceedingly narrow and therefore contributes negligibly to $\mathbf{D}(\mathbf{k}, q, \omega)$ and $\mathbf{Q}(\mathbf{k}, q, \omega)$: back-of-the-envelope estimates indicate that contributions to $\mathbf{D}(\mathbf{k}, q, \omega)$ and $\mathbf{Q}(\mathbf{k}, q, \omega)$ coming from the k'

sum over $[0, \omega/c_s]$ are $0(\omega^3 d^3/c_s^3)$ and $0(\omega d/c_s)$ smaller than their respective ‘‘quasistatic’’ counterparts (19) and (20). These negligibly small estimates, moreover, remain the same when $\beta_s(k', \omega)$ is replaced by k' for $k' \in [0, \omega/c_s]$. The approximate expressions (19) and (20) are especially well suited to those collective modes whose small- k oscillation frequencies are at most of the order of the bulk plasma frequency $\omega_p = (4\pi n_s e^2/m^* \epsilon_s d)^{1/2} \ll c_s/d$ (e.g., for a correlated GaAs superlattice with carrier density $n_s = 1.3 \times 10^{10} \text{ cm}^{-2}$ and $d = a = 495 \text{ \AA}$, $\omega_p = 0.0018 c_s/d$). Long-wavelength ($kd \ll 1$) plasmon and shear modes certainly fall in this category.

Further insight into the structure of \mathbf{D} and \mathbf{Q} can be gained by reformulating them in a way which explicitly features the intralayer (00) and interlayer ($\pm 10, \pm 20, \dots$) correlational contributions. This is accomplished by substituting Eq. (12) into Eqs. (19) and (20) and using Eq. (10). One readily obtains

$$\mathbf{D}(\mathbf{k}, q) = \mathbf{D}_{00}(\mathbf{k}) + \sum_{m \neq 0} \mathbf{D}_{m0}(\mathbf{k}, q), \quad (21)$$

$$\mathbf{Q}(\mathbf{k}, q, \omega) = \mathbf{Q}_{00}(\mathbf{k}, \omega) + \sum_{m \neq 0} \mathbf{Q}_{m0}(\mathbf{k}, q, \omega), \quad (22)$$

$$\mathbf{D}_{00}(\mathbf{k}) = \frac{1}{kN_e} \sum_{\mathbf{k}'} \mathbf{L}(\mathbf{k}') k' [S_{00}(|\mathbf{k} - \mathbf{k}'|) - S_{00}(k')], \quad (23)$$

$$\begin{aligned} \mathbf{D}_{m0}(\mathbf{k}, q) &= \frac{1}{kN_e} \sum_{\mathbf{k}'} \mathbf{L}(\mathbf{k}') k' e^{-k'|m|d} \\ &\times [S_{|m|0}(|\mathbf{k} - \mathbf{k}'|) \cos(qmd) - S_{|m|0}(k')], \end{aligned} \quad (24)$$

$$\mathbf{Q}_{00}(\mathbf{k}, \omega) = -\left(\frac{\omega}{c_s}\right)^2 \frac{1}{kN_e} \sum_{\mathbf{k}'} \mathbf{T}(\mathbf{k}') \frac{1}{k'} [S_{00}(|\mathbf{k} - \mathbf{k}'|) - 1], \quad (25)$$

$$\begin{aligned} \mathbf{Q}_{m0}(\mathbf{k}, q, \omega) &= -\left(\frac{\omega}{c_s}\right)^2 \frac{1}{kN_e} \sum_{\mathbf{k}'} \mathbf{T}(\mathbf{k}') \frac{1}{k'} e^{-k'|m|d} \\ &\times [S_{|m|0}(|\mathbf{k} - \mathbf{k}'|) \cos(qmd)]. \end{aligned} \quad (26)$$

The index notation $\mathbf{D}_{mn}(\mathbf{k}, q)$ was introduced to emphasize that a \mathbf{D}_{mn} term originates from the corresponding S_{mn} structure function. It does not imply that \mathbf{D}_{mn} is the m, n element of the \mathbf{D} matrix, if Eq. (5) is written down in layer-space representation [cf. Ref. 4(c)]

For the long-wavelength ($kd \ll 1$) plasmon and shear modes, it can also be shown that

$$\begin{aligned} |Q_{m0}^\alpha(kd \ll 1, q, \omega)| &= O(\omega^2/k^2 c_s^2) |D_{m0}^\alpha(kd \ll 1, q)| \\ &< (\omega_p^2/k^2 c_s^2) |D_{m0}^\alpha(kd \ll 1, q)|, \end{aligned} \quad (27)$$

$$\alpha = L, T; \quad m = 0, \pm 1, \pm 2, \dots$$

Consequently, $|Q_{m0}^\alpha(kd \ll 1, q, \omega)| \ll |D_{m0}^\alpha(kd \ll 1, q)|$, provided that $k^2 \gg \omega_p^2/c_s^2$. In the collective-mode analysis of Sec. IV, we therefore discard the electromagnetic-induced

correlational contributions (25) and (26) with the understanding that kd lies in the interval $(\omega_p d/c_s)^2 \ll k^2 d^2 \ll 1$ (we note that for semiconductor superlattices, the excluded interval $[0, \omega_p d/c_s]$ is exceedingly narrow). This is the underlying rationale for the so-called quasistatic approximation which formally amounts to setting c_s equal to infinity, so that $\beta_s(k, \omega) = k$, $Q^L(\mathbf{k}, q, \omega) = 0$, and $Q^T(\mathbf{k}, q, \omega) = 0$, and the dispersion analysis is thereby extended all the way down to $k = 0$.

In the small- kd regime, the quasistatic expressions for the longitudinal and transverse elements of Eqs. (23) and (24) become

$$D_{00}^\alpha(k \rightarrow 0) = (kd/2) J_{00}^\alpha, \quad (\alpha = L, T), \quad (28)$$

$$\begin{aligned} D_{m0}^\alpha(k \rightarrow 0, q) &= \frac{1}{2kd} [\cos(qmd) - 1] I_{|m|0} \\ &+ \frac{kd}{2} J_{|m|0}^\alpha \cos(qmd), \quad m = \pm 1, \pm 2, \dots \\ &(\alpha = L, T), \end{aligned} \quad (29)$$

$$J_{00}^L = \frac{5}{8N_e} \sum_{\mathbf{k}'} \frac{1}{k'd} [S_{00}(k') - 1] = -5J_{00}^T, \quad (30)$$

$$I_{|m|0} = \frac{1}{N_e} \sum_{\mathbf{k}'} (k'd) S_{|m|0}(k') e^{-k'|m|d}, \quad m = \pm 1, \pm 2, \dots \quad (31)$$

$$\begin{aligned} J_{|m|0}^L &= \frac{1}{8N_e} \sum_{\mathbf{k}'} \frac{1}{k'd} S_{|m|0}(k') \\ &\times e^{-k'|m|d} [5 - 11(k'|m|d) + 3(k'|m|d)^2], \\ &m = \pm 1, \pm 2, \dots, \end{aligned} \quad (32)$$

$$\begin{aligned} J_{|m|0}^T &= -\frac{1}{8N_e} \sum_{\mathbf{k}'} \frac{1}{k'd} S_{|m|0}(k') \\ &\times e^{-k'|m|d} [1 + (k'|m|d) - (k'|m|d)^2], \\ &m = \pm 1, \pm 2, \dots \end{aligned} \quad (33)$$

IV. COLLECTIVE MODES

Invoking the quasistatic approximation discussed above, Eqs. (15)–(17) or (18) provide the longitudinal (L) TM plasmon and the transverse (T) TE shear mode eigenfrequencies

$$\omega^2(\mathbf{k}, q) = \omega_{2D}^2(k) [F(k, q) + D^L(\mathbf{k}, q)] \quad (L), \quad (34)$$

$$\omega^2(\mathbf{k}, q) = \omega_{2D}^2(k) D^T(\mathbf{k}, q) \quad (T), \quad (35)$$

where $D^L(\mathbf{k}, q)$ and $D^T(\mathbf{k}, q)$ are the longitudinal and transverse elements of Eq. (19). The longitudinal mode can be identified as the well-known plasmon mode. The transverse excitation is a *shear mode* which is discussed here in detail for the first time, to our knowledge. Similar shear modes in the strongly coupled 3D OCP [Ref. 11(b)] and 2D electron liquid⁹ have been, however, identified earlier.

In the RPA limit, D^L and D^T are equal to zero, and only the plasmon modes survive. The RPA plasmon structure, which was extensively analyzed by Fetter,⁷ consists of an isolated bulk mode ($q=0$) and a band of acoustic modes with each mode labeled by a (nonzero) q value. Strong correlations, manifested by D^L and D^T being nonzero, modify the spectrum in two important ways. The first is the appearance of the shear mode, the second is the development of a finite frequency *energy gap* at $k=0$. We now proceed to discuss the plasmon and shear modes in the strongly correlated regime.

We will consider in detail the behavior of the mode dispersions in the long-wavelength ($kd < 1$) limit, which is of principal physical interest. In this domain, Eqs. (34) and (35) become to $O(k^2 d^2)$,

$$\begin{aligned} \omega^2(k \rightarrow 0, q) = & \omega_p^2 \frac{(kd)^2 [1 + \frac{1}{6}(kd)^2]}{2(1 - \cos qd) + (kd)^2 [1 + \frac{1}{12}(kd)^2]} \\ & + \frac{1}{4} \omega_p^2 (kd)^2 \sum_m J_{|m|0}^L \cos(qmd) \\ & + \frac{1}{4} \omega_p^2 \sum_{m \neq 0} [1 - \cos(qmd)] |I_{|m|0}| \quad (L), \quad (36) \end{aligned}$$

$$\begin{aligned} \omega^2(k \rightarrow 0, q) = & \frac{1}{4} \omega_p^2 (kd)^2 \sum_m J_{|m|0}^T \cos(qmd) \\ & + \frac{1}{4} \omega_p^2 \sum_{m \neq 0} [1 - \cos(qmd)] |I_{|m|0}| \quad (T), \quad (37) \end{aligned}$$

with the k - and q -independent coefficients I_{m0} , J_{00}^L , J_{00}^T , J_{m0}^L , and J_{m0}^T , given by Eqs. (30)–(33). Due to the isotropy of the liquid phase in the xy plane, at $k=0$ and $q \neq 0$ the ‘‘longitudinal’’ plasmon and ‘‘transverse’’ shear modes are degenerate: both of them develop the same energy gap.

$$\omega^2(0, q) = \frac{1}{2} \omega_p^2 \sum_{m \geq 1} [1 - \cos(qmd)] |I_{m0}| \quad (L, T). \quad (38)$$

This mode propagates in the z direction with its electric vector polarized in the lattice plane. Evidently interlayer correlations bring about a dramatic change in the behavior of the acoustic excitation spectrum: the small- k plasmon modes, which are acoustic ($\omega \propto k$) in the absence of interlayer correlations⁷ develop a finite energy gap at $k=0$,^{3,4(e),5,6} and lose their acoustic character. Physically, the mode can be portrayed as the shearlike oscillations of the adjacent layers with respect to each other. As has been discussed in greater detail in earlier publications,^{3,5,6} the physical explanation of the finite frequency of these oscillations (the energy gap) can be found by realizing that as long as the interlayer spacing d is not very much greater than the 2D Wigner-Seitz radius a , the state of the strongly correlated superlattice is hardly distinguishable from a slab in a (somewhat anisotropic) 3D Wigner crystal. In turn, the particle motion corresponding to the ‘‘acoustic’’ mode is not substantially different from that of a normal shear mode in a Wigner crystal propagating

along the superlattice axis with wave number q (of the order π/d). Since for small q , the shear mode dispersion is *acoustic in q* , viz.

$$\omega(0, q \rightarrow 0) = \frac{1}{2} \omega_p q d \left(\sum_{m \geq 1} m^2 |I_{m0}| \right)^{1/2}, \quad (39)$$

and q is different from zero, the oscillation frequency is different from zero too. Hence the energy gap.

We now proceed to analyze the behavior for finite but small k ($0 < kd \ll 1$) values. Consider first the in-phase ($q d = 0$) behavior: the $q=0$ situation represents a singular behavior for the plasmon mode. The mode is now a bulk plasmon mode with frequency

$$\omega^2(k \rightarrow 0, 0) = \omega_p^2 \left[1 + k^2 d^2 \left(\frac{1}{12} + \frac{1}{4} \sum_m J_{|m|0}^L \right) \right], \quad (L) \quad (40)$$

Equation (40) exhibits a positive RPA frequency shift $(kd)^2 \omega_p/24$ arising from the form factor $F(k, 0)$ in the $kd \ll 1$ limit. [Note the structural likeness to the $(kd)^2 \omega_p (a_B^*/4d)$ shift arising from the pressure gradient term in a hydrodynamic model⁷ of the zero temperature layered 2D electron gas.] The positive form factor dispersion is offset by the net negative correlational dispersion arising from the J_{m0}^L coefficients. Numerical calculations (see tabulations below) indicate that J_{00}^L is negative and that J_{10}^L is positive or negative and much smaller. For $\Gamma = 10$ and $d/a = 2$, the dispersion coefficient $\alpha = (\frac{1}{12} - \frac{1}{4} |\sum_m J_{|m|0}^L|) \approx 0.0023$; for $\Gamma = 20$ and $d/a = 2$, the positive dispersion decreases slightly to $\alpha \approx 0.0018$. The most significant effect occurs, however, when the interlayer coupling is increased (by decreasing d) to the point where it is comparable with the intralayer coupling: at $\Gamma = 10$ and $d/a = 1$, we calculate $\alpha \approx -0.0511$, indicating the onset of negative (crystal-like) dispersion quite similar to that of the strongly coupled 3D OCP.^{11(b)}

For $q \neq 0$ both the plasmon and the shear modes exhibit quadratic dispersion:

$$\omega^2(k \rightarrow 0, q \neq 0) = \omega^2(0, q) + V_{L,T}^2 k^2, \quad (L, T) \quad (41)$$

where the dispersion coefficients are given by

$$V_L^2 = \omega_p^2 d^2 \left\{ \frac{1}{2(1 - \cos qd)} + \frac{1}{4} \sum_m J_{|m|0}^L \cos(qmd) \right\} \quad (L), \quad (42)$$

$$V_T^2 = \omega_p^2 d^2 \frac{1}{4} \sum_m J_{|m|0}^T \cos(qmd) \quad (T) \quad (43)$$

The calculations of the energy gap frequency (38) and the long-wavelength oscillation frequencies (36) and (37) require a knowledge of the intralayer and interlayer static structure functions $S_{00}(k)$ and $S_{m0}(k)$. To recount what has been accomplished thus far in the way of numerical calculations, the plasmon and shear mode dispersion curves of Refs. 4(e) and 6 were generated on the assumption that the first \mathbf{D}_{00} and \mathbf{D}_{10} terms in Eq. (21) are the dominant contributions to $\mathbf{D}(k \rightarrow 0, q)$, so that only $S_{00}(k)$ and $S_{10}(k)$ are required. These latter were calculated using the iterative weak (inter-

layer) correlations—strong-(intralayer) coupling (WCSC) approximation scheme, originally suggested by Kalman, Ren, and Golden.⁵ The WCSC calculation requires the static structure function for the isolated 2D layer as an input which is available both for the zero-temperature electron liquid¹⁸ and for the classical electron liquid.^{19–21} The iterative program can be carried out in a straightforward fashion for the superlattice modeled as a classical system, but would require drastic additional approximations involving the *dynamical* structure function for the fully degenerate electron liquid. Therefore, in order to portray best the influences of both interlayer and intralayer correlations, the gapped plasmon and shear mode WCSC calculations of Refs. 4(e), 5, and 6 and this paper are based on the classical superlattice model characterized by the coupling parameter Γ . The $k=0$ energy gap for the out-of-phase ($qd = \pm\pi$) plasma mode is displayed graphically in Ref. 5 as a function of d/a for values of Γ up to 22. The band of “gapped” plasmon dispersion curves calculated from Eq. (36) for $m=0$ and ± 1 are displayed in Ref. 4(e) for $\Gamma=10$ and $d/a=1$ and in Ref. 10 for $(\Gamma, d/a)$ values of (1,1) and (10,2). The companion band of gapped shear mode dispersion curves calculated from Eq. (37) are displayed in the present work in Fig. 1(a)–1(c) for $(\Gamma, d/a)$ values of (10,1), (10,2), and (20,2). These dispersion curves are generated from the Eqs. (30)–(33) I and J coefficients, which in the WCSC approximation, are calculated in Table I. The $\Gamma=10$ value corresponds to $r_s=5$, and is therefore applicable to a GaAs superlattice (substrate dielectric constant $\epsilon_s=13.1$, effective mass $m^*=0.07m_e$, effective Bohr radius $a_B^*=99 \text{ \AA}$) with carrier density $n_s=1.3 \times 10^{10} \text{ cm}^{-2}$. There is a substantial reduction in the magnitude of the energy gap as d/a increases from 1 to 2 for $\Gamma=10$: $\omega(k=0, q=\pm\pi/d)=0.423\omega_p$ for $d/a=1$ and $\omega(k=0, q=\pm\pi/d)=0.067\omega_p$ for $d/a=2$. Interestingly enough, we also report a small decrease in the gap as Γ increases from 10 to 20 for fixed $d/a=2$: $\omega(k=0, q=\pm\pi/d)=0.0677\omega_p$ for $\Gamma=10$ and $\omega(k=0, q=\pm\pi/d)=0.0588\omega_p$ for $\Gamma=20$. This too is consistent with the calculations of Ref. 5. As in the case of the plasmon band,⁶ interlayer correlations bring about dramatic modifications in the shear mode dispersion. In fact the effect on the shear band is even more dramatic. Comparison of Figs. 1(a) and 1(b) shows how the decrease in interlayer coupling with increasing d/a (for fixed Γ) substantially lowers the energy gap value and compresses the shear mode band. This compression becomes more and more pronounced with increasing d/a until the band eventually collapses into a single 2D acoustic shear mode in the zero interlayer coupling limit, i.e., at $S_{10}(k)=0$. In this limit Eq. (37) simplifies to $\omega^2=1/2\omega_p^2(kd)^2J_{00}^T$. The energy gap also collapses as qd approaches zero. In contrast to the plasmon mode, which, as discussed above, develops in this case a singular behavior, the shear mode goes over smoothly into bulk shear behavior, where all the layers execute an in-phase transverse oscillation. This behavior is now strictly acoustic with the frequency

$$\omega^2(k \rightarrow 0, 0) = \frac{1}{4}\omega_p^2(kd)^2 \sum_m J_{|m|0}^T(T). \quad (44)$$

For coefficients (30) and (33), Table I shows J_{00}^T to be positive and dominant; for $d/a=1$, the much smaller negative

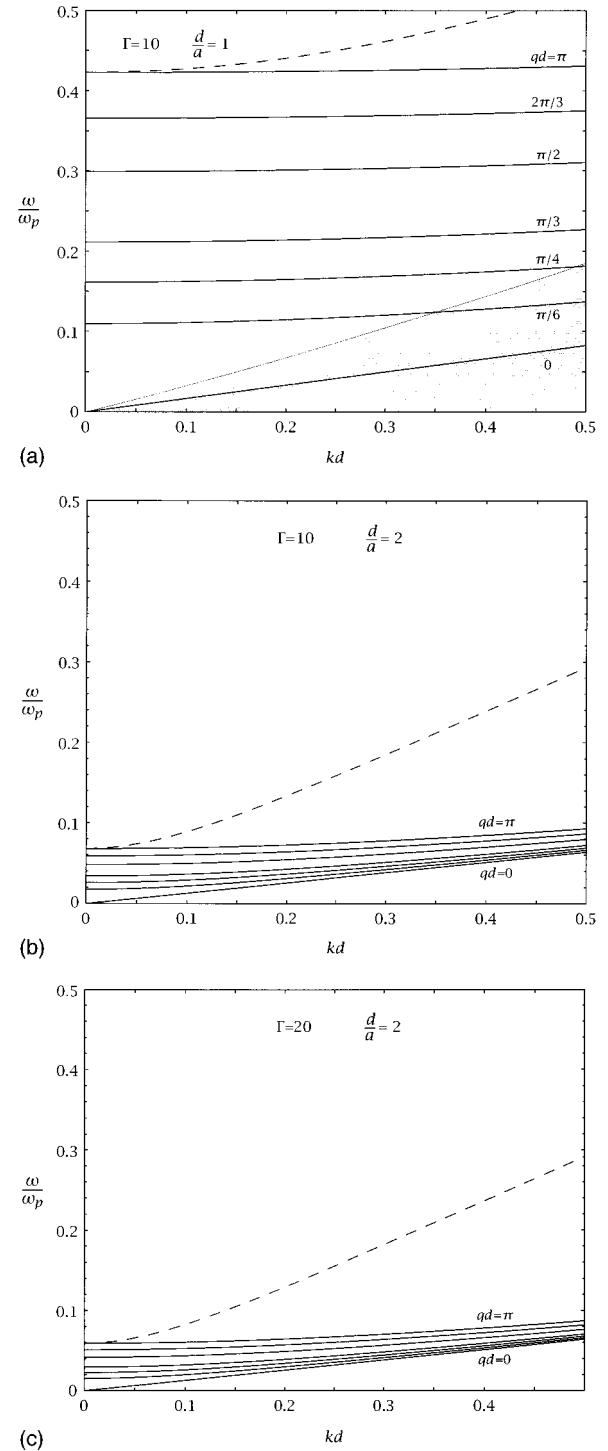


FIG. 1. (a)–(c) Shear mode dispersion curves calculated from Eq. (37) for $(\Gamma, d/a) = (10, 1)$, $(10, 2)$, and $(20, 2)$. The modes are labeled by qd values; $\omega_p^2 = 4\pi n_s e^2 / (dm^* \epsilon_s)$. The $S_{00}(k)$ and $S_{10}(k)$ structure functions in Eqs. (30)–(33) were calculated in the Ref. 5 WCSC approximation using as input the hypernetted chain data of Ref. 21. The longitudinal plasmon modes are also shown (as dashed lines) for comparison at $qd = \pi$. The shaded region in (a) is the pair continuum.

J_{10}^T acts to slightly offset the intralayer correlational coefficient. Additionally, our calculations indicate that for $r_s < 18$ (corresponding to $\Gamma < 36$), the in-phase gapless mode will always lie inside the pair continuum [see, e.g., Fig. 1(a)], and

TABLE I. Calculated I_{10} , J_{00} , and J_{10} values based on the WCSC approximation (Ref. 5), using the HNC data of Ref. 21

Γ	d/a	I_{10}	J_{00}^L	J_{10}^L	J_{00}^T	J_{10}^T
10	1	-0.179	-0.557	9.86×10^{-3}	0.111	-1.51×10^{-3}
10	2	-4.59×10^{-3}	-0.324	6.13×10^{-5}	0.0648	5.50×10^{-5}
20	2	-3.46×10^{-3}	-0.326	-3.79×10^{-5}	0.0652	-5.04×10^{-5}

is therefore heavily Landau damped. Most of the gapped shear modes, however, are not (see below).

A word of caution concerning the $qd \rightarrow 0$ limit is in order: when this limit is reached by letting $d \rightarrow 0$, the above limiting process implies that the phase difference (qd) between neighboring layers also goes to zero as the distance between them is diminished. Another possible limit can, however, arise by keeping the phase $qd = \text{const}$ as $d \rightarrow 0$. This corresponds to a different physical situation (of interest, primarily for a finite number of layers), and is not discussed here any further.

The problem of observability both of the shear mode and of the plasmon gap leads to two closely related, nevertheless distinct, questions: first, how reliable are the predictions of the QLC approximation, and, second, what is the damping of these modes? As to the first, one should recall that the principal assumption upon which the QLCA is built is that the migration-diffusion time of the particles away from their instantaneous position is long enough to justify the description of the system in terms of its static configuration. An upper limit on this migration-diffusion time τ_D can be set by using the result of Hansen, Levesque, and Weis,²² who obtained a value for the self-diffusion coefficient of a 2D classical electron gas through molecular-dynamics simulation. Let $\tau_D = \lambda^2/D$ be the diffusion time with D the self-diffusion coefficient, and λ the migration distance of a particle from its quasisite position sufficient to destroy local order. The behavior of D can be inferred from the data of Ref. 22: we calculate $D \approx 5a^2\omega_0/\Gamma^{1.3}$ and $\omega_{\min} = \tau_D^{-1} = (2.5/\Gamma^{1.3}) \times (d/a)^{1/2}(a/\lambda)^2\omega_p$, where $\omega_0^2 = e^2/(ma^3)$. ω_{\min} is clearly the frequency below which the QLC treatment is not justified. For $\Gamma=10$ and $d/a=1$, this order-of-magnitude estimate provides $\omega_{\min} \approx [a^2/(8\lambda^2)]\omega_p$; it can be compared with the corresponding $\omega(k=0, q=\pi/d) = 0.42\omega_p$ energy gap, indicating a borderline situation. For $\Gamma=10$ and 20 when $d/a=2$ the situation worsens because of the much smaller energy gaps. On the other hand, for $d/a=1$ and at Γ values $\Gamma \geq 40$, where ω_{\min} is much smaller, and where the out-of-phase $k=0$ gap frequency is expected to be at least as large as the $\Gamma=10$ gap value of $0.42\omega_p$,⁵ most of the gapped shear modes should exist: e.g., $\omega_{\min} \approx 10^{-2}(a/\lambda)^2\omega_p$ at $\Gamma=50$ (corresponding to $r_s=25$ for type-I multilayer hole structures with carrier densities $=1.3 \times 10^{10} \text{ cm}^{-2}$) and $d/a=1$.

The above estimation of the inverse migration-diffusion time as limited only by the classical electron-electron correlations is clearly an overestimate. In a realistic situation, other effects are expected to slow down the process considerably. In fact, the electron liquid exists in the presence of (static and dynamic) random fields, and the diffusion process is dominated by this disorder. The details of the localization and delocalization (i.e., migration) under the combined influence of disorder and strong coupling are not well understood

(for a recent review, see Ref. 23). What can, however, be expected with confidence is that the physical migration-diffusion time even in high-mobility samples would be sufficiently longer than the one determined from the classical self-diffusion coefficient. Since this latter estimate has already led to a borderline situation, one could assume that the QLCA can reasonably be used down to the characteristic gap frequencies.

The second aspect that one has to consider in order to assess the observability of the mode structure predicted is the actual damping of these modes. The two primary mechanisms for damping are decay by pair excitations (Landau damping) and impurity scattering. It is well known that even within the RPA description (where the $k=0$ gap is absent) the acoustic plasmon, because of its high phase velocity ($v_{\text{ph}} > v_F$), lies outside the pair continuum and is not affected by Landau damping. The existence of the gap renders this scenario even more pronounced. The shear mode, on the other hand, can have a low phase velocity ($v_{\text{ph}} < v_F$ for $r_s < 18$) and would be heavily Landau damped, were it not for the energy gap. Figure 1(a) shows that a gapped shear mode penetrates the pair continuum only for $k > k_*$, where k_*d , while depending both on q and d/a , ranges from 0.35 to 0.49 for $\pi/6 \leq qd \leq \pi/4$; modes with qd values in the interval $(\pi/4, \pi]$ lie above the pair continuum for $kd < 0.5$. Thus one can conclude that Landau damping should not seriously affect the long wavelength mode propagation.

Turning now to impurity scattering, we note that modern nanotechnology has made extremely high-mobility samples available, where the effect of impurity scattering (including electron-phonon scattering) has been dramatically reduced, even at low carrier densities. Using recent data from measurements by Pfeiffer *et al.*,²⁴ where $\mu \approx 1.5 \times 10^6 \text{ cm}^2/\text{V}$ was reported at $n_s = 2 \times 10^{10} \text{ cm}^{-2}$, one can calculate an effective collision frequency $\nu \approx 1.7 \times 10^{10} \text{ s}^{-1}$. This can be compared with a typical out-of-phase gap frequency $0.42\omega_p$ quoted above, with $\omega_p = 3.7 \times 10^{12} \text{ s}^{-1}$. Thus impurity scattering also does not seem to cause a major modification of the mode structure.

V. ANISOTROPIC MEDIUM DESCRIPTION

In the combined $kd \rightarrow 0$ and $qd \rightarrow 0$ limit the infinite superlattice is equivalent to a homogeneous anisotropic medium; the isotropy is broken along the z direction, due to the inhibited particle motion along this direction. A medium with this kind of anisotropy and with a \mathbf{k} vector along the x direction can be described in terms of a 3D dielectric tensor $\bar{\epsilon}$ with nonvanishing elements $\bar{\epsilon}_{xx} = \bar{\epsilon}_L$, $\bar{\epsilon}_{yy} = \bar{\epsilon}_T$, and $\bar{\epsilon}_{zz} = 1$ (the barred notation is used to distinguish the 3D $\bar{\epsilon}$ from the previously used superlattice ϵ). In turn, $\bar{\epsilon}_L$ and $\bar{\epsilon}_T$ may be obtained from the appropriate 3D expressions of Ref.

11(b), with the understanding that $\omega_p^2 D_L$ and $\omega_p^2 D_T$ therein are to be replaced by $\omega_{2D}^2(k) D^L(\mathbf{k}, q)$ and $\omega_{2D}(k) D^T(\mathbf{k}, q)$ from Eq. (15), respectively:

$$\bar{\epsilon}^{L,T}(\mathbf{k}, q, \omega) = \epsilon_s \left\{ 1 - \frac{\omega_p^2}{\omega^2 - \omega_{2D}^2(k) D^{L,T}(k, q)} \right\}, \quad (45)$$

The collective modes are now determined through the 3D dispersion relation with k and q considered as the components of a 3D propagation vector $\mathbf{K} = \mathbf{k} + \hat{e}_z q$:

$$\left| \bar{\epsilon}(\mathbf{k}, q, \omega) - \frac{(k^2 + q^2) c_s^2}{\omega^2} \mathbf{T}(\mathbf{K}) \right| = 0. \quad (46)$$

Equation (46) leads to the longitudinal and transverse relations

$$\bar{\epsilon}_L(\mathbf{k}, q, \omega) = \frac{q^2 c_s^2}{\omega^2 - k^2 c_s^2} \quad (L), \quad (47)$$

$$\bar{\epsilon}_T(\mathbf{k}, q, \omega) = \frac{(k^2 + q^2) c_s^2}{\omega^2} \quad (T). \quad (48)$$

Each of these equations describes, thus, a high-frequency and a low-frequency mode. It is the latter that are of interest to us. In the quasistatic approximation these latter become

$$\omega^2(\mathbf{k}, q) = \omega_p^2 \frac{k^2}{k^2 + q^2} + \omega_{2D}^2(k) D^L(\mathbf{k}, q) \quad (L) \quad (49)$$

and

$$\omega^2(\mathbf{k}, q) = \omega_{2D}^2(k) D^T(\mathbf{k}, q) \quad (T). \quad (50)$$

These are identical to the small- k and small- q expansions of Eqs. (36) and (37).

VI. CONCLUSIONS

In this paper we calculated the dynamical matrix and dielectric response tensor for the correlated superlattice in the quasilocalized charge approximation. The intralayer and interlayer correlational effects are embodied in expressions (11) and (14) for $\mathbf{D}(\mathbf{k}, q, \omega)$ and $\mathbf{Q}(\mathbf{k}, q, \omega)$, whose longitudinal and transverse elements appear as static local-field corrections in the QLC dielectric tensor elements [portrayed by Eq. (15)]. We formulated the TM and TE dispersion relations

in the quasilocalized charge approximation, and analyzed them in the long-wavelength ($kd \ll 1$) regime to determine how Coulomb correlations modify the RPA collective mode structure. The principal results of this work are represented by Eqs. (15) and (18) for the QLC dielectric tensor elements and dispersion relation, respectively, and by Eqs. (36), (37), and (40)–(43), and Figs. 1(a)–1(c) for the shear mode dispersion.

Our analysis of the TM and TE dispersion relations in the quasistatic limit shows that the QLCA collective-mode structure consists of (i) an in-phase ($q=0$) longitudinal plasmon which exhibits crystal-like dispersion at long wavelengths for sufficiently strong interlayer coupling [Eq. (40)]; (ii) the band of gapped plasmon modes [Eq. (36)] reported in Ref. 6; (iii) an in-phase transverse shear mode which exhibits acoustic-phonon-like dispersion at long wavelengths [Eq. (44)], and (iv) a band of gapped shear modes [Eq. (37), Figs. 1(a)–1(c)]. The $k=0$ gap frequency (38) and the shear mode band (37) share one common feature: both are wholly maintained by non-RPA interlayer correlations. When interlayer correlations are suppressed, i.e., when the mutual Coulomb interaction of the layers is taken into account through the average RPA field only, the in-phase mode (iii) and the band (iv) merge into a single 2D isolated layer shear mode⁹ which is wholly maintained by intralayer correlations.

Since there are no other sources of $S_{10}(k)$ data available at the present time save the WCSC iterative scheme⁵ which breaks down for $\Gamma > 22$, the lack of $S_{10}(k)$ data at higher- Γ values precludes the possibility of generating dispersion curves with high gap values. Nevertheless, the $k=0$ energy gap frequency of $0.42\omega_p$ calculated from the WCSC data for $\Gamma=10$, $d/a=1$ can be considered to be a reliable lower-bound estimate for the out-of-phase plasmon and shear mode oscillation frequencies in the coupling regimes where these and most of the lower- q gapped shear modes are expected to be undamped.

ACKNOWLEDGMENTS

This work was partially supported by NSF Grant Nos. PHY-9115615 and PHY-9115714. Part of the work was done while K.I.G. was a visitor at the Australian National University Institute of Advanced Studies' Department of Theoretical Physics, where he had numerous useful discussions with Mukunda P. Das.

¹C. Zhang and N. Tzoar, Phys. Rev. A **38**, 5786 (1988).

²L. Swierkowski, D. Neilson, and J. Szymanski, Aus. J. Phys. **46**, 423 (1993); D. Neilson, L. Swierkowski, J. Szymanski, and L. Liu, Phys. Rev. Lett. **71**, 4035 (1993); **72**, 2669(E) (1994).

³K. I. Golden and G. Kalman, Phys. Status Solidi B **180**, 533 (1993).

⁴(a) G. Kalman and K. I. Golden, in *Condensed Matter Theories 8*, edited by L. Blum and B. Malik (Plenum, New York, 1993), pp. 127–135; (b) G. Kalman, Y. Ren, and K. I. Golden, in *Proceedings of VI International Workshop on the Physics of Nonideal Plasmas*, edited by T. Bornath and W. D. Kraeft [Contrib. Plasma Phys. **33**, 449 (1993)]; (c) G. Kalman and K. I. Golden,

in *Condensed Matter Theories 9*, edited by J. W. Clark, K. A. Hoab, and A. Sadiq (Nova, New York, 1994), pp. 123–135; (d) K. I. Golden, in *Modern Perspectives in Many-Body Theory*, edited by M. P. Das and J. Mahanty (World Scientific, Singapore, 1994), pp. 315–346; (e) K. I. Golden, L. Miao, and G. Kalman, in *Proceedings of the International Conference on the Physics of Strongly Coupled Plasmas*, edited by W. Kraeft and M. Schlanges (World Scientific, Singapore, 1996), pp. 409–418.

⁵G. Kalman, Y. Ren, and K. I. Golden, Phys. Rev. B **50**, 2031 (1994).

⁶Dexin Lu, K. I. Golden, G. Kalman, Ph. Wyns, L. Miao, and X.-L. Shi, Phys. Rev. B **54**, 11 457 (1996).

- ⁷A. L. Fetter, *Ann. Phys. (N.Y.)* **88**, 1 (1974).
- ⁸(a) G. Goldoni and F. M. Peeters, *Phys. Rev. B* **53**, 4591 (1995);
(b) D. H. Dubin (unpublished); (c) K. Esfarjani and Y. Kawazoe, *J. Phys. Condens. Matter* **7**, 7217 (1995).
- ⁹K. I. Golden, G. Kalman, and Ph. Wyns, *Phys. Rev. A* **46**, 3463 (1992).
- ¹⁰G. Kalman and K. I. Golden, *Phys. Rev. A* **41**, 5516 (1990).
- ¹¹(a) K. I. Golden, G. Kalman, and Ph. Wyns, *Phys. Rev. A* **41**, 6940 (1990); (b) **46**, 3454 (1992); (c) *Phys. Rev. B* **48**, 8882 (1993).
- ¹²K. I. Golden, G. Kalman, and L. Miao (unpublished)
- ¹³R. D. King-Smith and J. C. Inkson, *Phys. Rev. B* **36**, 4796 (1987).
- ¹⁴K. I. Golden and Dexin Lu, *Phys. Rev. A* **45**, 1084 (1992); *Phys. Rev. E* **47**, 4632 (E) (1993).
- ¹⁵J.-P. Hansen, I. R. McDonald, and E. L. Pollock, *Phys. Rev. A* **11**, 1025 (1975).
- ¹⁶P. Carini, G. Kalman, and K. I. Golden, *Phys. Lett.* **78A**, 450 (1980); P. Carini and G. Kalman, *ibid.*, **105A**, 229 (1984).
- ¹⁷K. I. Golden and G. Kalman, *Phys. Rev. B* **52**, 14 719 (1995).
- ¹⁸B. Tanatar and D. M. Ceperley, *Phys. Rev. B* **39**, 5005 (1989).
- ¹⁹H. Totsuji, *Phys. Rev. A* **17**, 399 (1978).
- ²⁰R. S. Gann, S. Chakravarty, and G. V. Chester, *Phys. Rev. B* **20**, 326 (1979).
- ²¹F. Lado, *Phys. Rev. B* **17**, 2827 (1978).
- ²²J. P. Hansen, D. Levesque, and J. J. Weis, *Phys. Rev. Lett.* **43**, 979 (1979).
- ²³D. Belitz and T. R. Kirkpatrick, *Rev. Mod. Phys.* **66**, 261 (1994).
- ²⁴L. Pfeiffer, K. V. Vest, H. L. Stormer, and K. W. Baldwin, *Appl. Phys. Lett.* **55**, 1888 (1989).